RESEARCH ARTICLE

Aryl-group substituted polysiloxanes with high-optical transmission, thermal stability, and refractive index

Dennis Meier | Volker Huch [ID] | Guido Kickelbick [ID]

Inorganic Solid-State Chemistry, Saarland University, Saarbrücken, Germany

Correspondence
Guido Kickelbick, Saarland University, Inorganic Solid-State Chemistry, Campus Building C4 1, 66123 Saarbrücken, Germany.
Email: guido.kickelbick@uni-saarland.de

Abstract

Polysiloxanes are an important class of polymers for optoelectronic applications. Novel polysiloxanes with high-refractive index (RI) based on phenanthrenyl-substituted monomers are prepared by a polycondensation reaction starting from various substituted dialkoxysilanes as monomers. The substitution patterns on the Si atom are systematically changed to vary the properties of the linear polymers as well as the final cured material. The two monomers with polycyclic aromatic side groups 9-phenanthrenylmethyldimethoxysilane and 9-phenanthrenylphenyldimethoxysilane are synthesized and fully characterized, including their single crystal X-ray structures. Linear polysiloxanes with variations in hydride, methyl, vinyl, phenyl, and phenanthrenyl side group content are prepared by acid- and base-catalyzed polycondensation reactions. Both Si—H and Si vinyl substituted polymers with molecular weights up to 30 kDa and adjustable RI's from 1.52 to 1.63 are obtained and the thermally cured by Pt-catalyzed hydrosilylation reactions. Polysiloxane resins are obtained with high-RI's, optical transmittance above 95% and thermal stabilities up to 420°C. Long-term thermal stability tests show transmittance values above 85% even after 60 days of thermal treatment at 180°C.

KEYWORDS

alkoxysilanes, high-refractive index, optical polymers, polycondensation, polysiloxanes, thermal stability

1 | INTRODUCTION

In recent years polysiloxanes show a renaissance in research due to their unique properties for optical applications, such as LED packaging, solar cells, or electrical memories.[1] Particularly their high-optical transparency in the visible range, their chemical inertness, high-thermal stability, excellent resistance to irradiation degradation, and outstanding processability makes them ideal materials for optoelectronic devices.[1–3] An important

parameter for many devices is a tailorable refractive index (RI) controlled by the substitution pattern in the polysiloxane backbone. In LED encapsulants this allows, for example, the fabrication of brighter LEDs. According to Snell's laws, the RI difference between the LED chip (e.g., GaN n = 2.5) and the encapsulation material leads to a very narrow light decoupling angle,[3,4] resulting in low-output power, as calculated by Schubert[5] and shown by Mosley et al.[6] The amount of light outcoupling, assuming that the light is emitted isotropically, can be
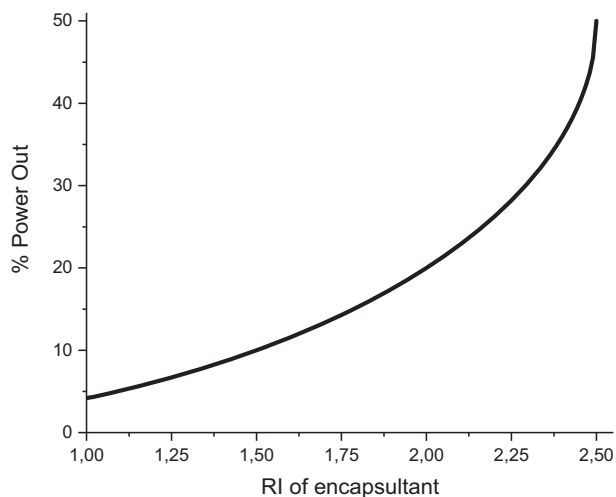
FIGURE 1 Ideal integrated power out of idealized surface of a hemisphere "point-like" chip with no secondary scattering

calculated using equation (Equation (1)), where Φ_{ca} is the critical angle, P_{escape} is the emitted photons and P_{source} is the generated photons of the GaN chip as a function of the RI of the encapsulation material (Figure 1). Small increases in RI result in a large increase in light extraction efficiency when the RI is above 1.5.

$$\frac{P_{escape}}{P_{source}} = \frac{1}{2}(1 - \cos\phi_{ca}). \tag{1}$$

The usually low RI of polysiloxanes leads to a backscattering of emitted photons into the chip, resulting in higher operating temperatures, reduced emission of photons,[5] and overall reduced lifetime of the polysiloxane. High-energy photons and high temperatures induce free radicals that degenerate the polysiloxanes and lead to yellowing.[7] For a more efficient light output the RI of the encapsulation material must be increased. In case of polysiloxanes the RI is influenced by the substitution pattern at the silicon atoms. By means of the Lorentz-Lorenz equation (Equation (2)), the RI of a substance or group can be related to its polarizability, which allows to estimate the effects of substitution pattern changes.[3,8,9] In this equation RI equals the molar refraction of the group and V_i the molar volume. Krevelen and Nijenhuis listed these values for plenty of chemical groups.[9] Furthermore, LED encapsulants also require a high-thermal stability in the range of 150 up to 270°C[10] and a high-optical transmittance above 95%.

$$\frac{n^2 - 1}{n^2 + 2} = \frac{\sum_i R_i}{\sum_i V_i}. \tag{2}$$

In literature, several approaches toward increased RIs retaining high-temperature stability are already

described for polysiloxanes. Mosley et al.[8] developed a polysiloxane with phenoxyphenyl side-groups to achieve a RI of 1.62 while keeping a transmittance of 97–99%. The use of phenylthiophenyl led to an even higher RI of 1.64 but a decrease of transmittance. Bae et al. developed a polydiphenylsiloxane (PDPS) with an increased RI of approximately 1.58 and a transmittance of approximately 90% at 450 nm.[11] Other improvements were generated by implementing epoxy groups in PDPS to increase adhesion and decrease viscosity for better processable polymers.[12,13] Increasing the amount of phenyl side-groups of polymethyl-phenylsiloxane raises the viscosity and RI,[14] while increasing the amount of cross-linking fosters its hardness, viscosity, and consequently decreases the moisture uptake.[15] Nanoparticle incorporation into the polymer matrix is another method to influence the RI.[16] But in many cases nanoparticle incorporation leads to a decrease of the thermostability.[17–24]

Increasing the number of aromatic groups in the polysiloxane backbone and extending the aromatic system can also increase the RI. Polysiloxanes with polycyclic aromatic groups have been known since 1984.[25] Beside the earlier reported phenoxyphenyl groups, biphenyl, and naphthyl groups[25,26] were introduced into polysiloxanes for Fe^{3+} ion sensing[26] or gas chromatography columns.[25] In recent years, polysiloxanes with polycyclic aromatic groups, such as anthracenyl[27] or pyrenyl[28] were synthesized and used as fluorescence markers[27] or as precursors in the synthesis of single walled-nanotubes via ball milling.[28]

In our study, linear polysiloxanes with polycyclic aromatic side groups were synthesized and their composition was systematically varied to investigate its influence on the RI. The polymers were cross-linked by Pt catalyzed hydrosilylation. The derived resins were investigated regarding influences of the composition of the pre-polymers on the final RI and the thermal stability.

2 | EXPERIMENTAL

2.1 | Materials

Diphenylsilandiole (97%), dimethyldimethoxysilane (MM) (97%), phenyl-trimethoxysilane (97%), methyltrimethoxysilane (97%), 9-bromophenanthrene (98%), and tetra-n-butylammonium hydroxide (40% solution on H_2O) were purchased from Alfa Aesar (Germany). Tert-butyldimethylchlorosilane (98%) was purchased from TCI America. 9-Bromophenanthrene (98%) and vinylphenyl-diethoxysilane (VP) (97%) were purchased from Fluorochem Ltd. (UK). Methylphenyl-dimethoxysilane (97%), methyldiethoxysilane (HM) (97%), and platinum

carbonyl cyclovinyl-methylsiloxane complex ("Ossko Catalyst") were purchased from ABCR (Germany). Xylene mixture (97%) was purchased from VWR International. Concentrated hydrochloric acid, magnesium chippings, as well as all solvents besides dry tetrahydrofuran (THF) were purchased from the Central Chemical Depot of Saarland University. THF (97%) was purchased from Fisher Scientific and purified via a solvent purification system MB-SPS-800 from M.Braun (Germany). Triethylamine was dried over calcium hydride and distilled prior to use. All other chemicals were used as received.

2.2 | Characterization

Fourier transform infrared (FTIR) measurements were performed under ambient air in attenuated total reflectance mode (ATR, 40 scans at a resolution of 4 cm^{-1}) on a Vertex 70 spectrometer (Bruker Optics, Germany). Thermogravimetric analyses (TGA) of the samples were measured on a TG 209C Iris (Netzsch Group, Germany) with 10 K min^{-1} heating rate and 40 ml min^{-1} nitrogen for the inert measurements and 20 ml min^{-1} oxygen and 20 ml min^{-1} nitrogen for the oxidizing measurements. Samples were measured up to 1000°C, while for both methods from 900 to 1000°C oxidizing atmosphere was used. Onset temperatures were established using 5% mass loss method, which is equivalent to 95% residual mass. Elemental analyses were performed with a 900 CHN analyzer (LECO, Germany). Differential scanning calorimetry (DSC) was recorded using a DSC 204 F1 Phoenix (Netzsch Group, Germany) with 10 K min^{-1} heating and a cooling rate from −60 to 150°C using liquid and gaseous nitrogen for cooling and 60 ml min^{-1} nitrogen as inert gas. RI's were measured at 622 nm using an Abbé refractometer (A. KRÜSS Optronic GmbH, Germany) at 20°C and monobromo-naphthaline as contact fluid for solid samples. UV/Vis spectra were recorded using a Lambda 750 (Perkin Elmer, UK) and a 100 mm integrating sphere, where the glass slide with the cured polysiloxane on top of it is located in front of the integrating sphere. For the transmission experiment, the sphere was closed, while for the diffusion experiment, which is needed to calculate the haze values, the primary light trap was open. The whiteness and yellowness indices were calculated using PerkinElmer UV Winlab (6.4.0.973) software. NMR measurements were recorded either on a Avance III HD 300 MHz or on a Avance III HD 400 MHz (both Bruker Corporation, USA) using chloroform-d as solvent and reference. The solid-state CP/MAS NMR spectra were recorded on a Avance III HD with an Ascend 400 WB (400 MHz) core (Bruker Corporation, USA) using a zirconia 4 mm rotor with 13 kHz rotation speed. Gel

permeation chromatography (SEC) was measured using a Viscotek VE1121 Pump (Malvern Panalytical, UK), two PSS SDV 10^3 and 10^5 columns (PSS Polymer Standards Service GmbH, Germany). Three detectors were used, a Shodex RID org udc 2 (RI, Showa Denko K.K. Japan), a UV 2487 (UV/Vis, Waters Corporation, USA) and a PSS SLD 7000/BI-MwA (light scattering, PSS Polymer Standards Service GmbH, Germany). Measurements were carried out in THF, calibrated with polystyrene standards using WinSEC 7 software. Plasma etching was carried out applying a Plasma-Surface-Technology Femto (Diener electronic GmbH + Co. KG, Germany) with 15 ml min^{-1} oxygen and 100% power for 15 min. Single crystal X-ray diffraction analysis were carried out on a Bruker AXS X8 Apex CCD diffractometer operating with graphite monochromated Mo Kα radiation. CCDC 2073540 and 2073539 contains the supplementary crystallographic data for the single crystal X-ray structures in the paper. These data can be obtained free of charge from The Cambridge Crystallographic Data Centre via www.ccdc.cam.ac.uk/structures.

2.3 | Monomer synthesis

Both syntheses are based on published procedures of Mosley et al.[8] and Kondo et al.[29,30]

2.3.1 | 9-Phenanthrenylmethyldimethoxy-silane

Magnesium chippings (2.00 g, 82.29 mmol) were added in dry THF (40 ml). A solution of 9-bromophenanthrene (20.00 g, 77.78 mmol) in dry THF (100 ml) was slowly added at room temperature and stirred for 1 h under reflux. In a second flask methyltrimethoxysilane (52.97 g, 388.9 mmol) in dry THF (50 ml) was mixed. The Grignard suspension of flask one was transferred into a dropping funnel of flask two via a transfer cannula. The suspension was slowly added to the mixture. After stirring the mixture at room temperature overnight it was heated under reflux for 1 h. The cooled suspension was filtered over a glass filter and the solvent was evaporated. The residue was suspended in toluene (200 ml) and filtered. After removing the solvent and the remaining methyltrimethoxysilane the raw product was distilled under vacuum (8 × 10^{-3} mbar, 152°C). Yield: 11.61 g (53%) colorless liquid.

^{1}H NMR (300.13 MHz, CDCl$_3$, δ): 8.84 (d, J = 7.6 Hz, 1H), 8.78 (d, J = 7.9 Hz, 1H), 8.57 (d, J = 7.9 Hz, 1H), 8.43 (s, 1H), 8.08 (d, J = 7.6 Hz, 1H), 7.79 (m, 4H), 3.82 (s, 6H), 0.73 (s, 3H); ^{13}C NMR (75.47 MHz, CDCl$_3$, δ): 137.75, 134.57, 131.55, 131.04, 130.66, 130.11, 129.27, 128.65, 127.73, 126.90, 126.68, 126.37, 123.17, 122.53, 50.62, −3.59; ^{29}Si NMR

(59.63 MHz, CDCl$_3$, δ): −13.12; Anal. calc. For C$_{17}$H$_{18}$O$_2$Si: C 72.32, H 6.45, N 0.00; found: C 72.30, H 6.42, N 0.00.

2.3.2 | 9-Phenanthrenylphenyldimethoxysilane

Magnesium chippings (2.00 g, 82.29 mmol) were added to dry THF (40 ml). A solution of 9-bromophenanthrene (20.00 g, 77.78 mmol) in dry THF (100 ml) was slowly added at room temperature and stirred for 1 h under reflux. In a second flask methyltrimethoxysilane (30.85 g, 155.56 mmol) in dry THF (50 ml) was mixed. The Grignard suspension of flask one was transferred into a dropping funnel of flask two via transfer cannula and slowly dropped into the flask. After stirring the mixture at room temperature overnight it was heated under reflux for 1 h. The cooled suspension was filtered over a glass filter and the solvent was evaporated. The residue was suspended in of toluene (200 ml) and filtered again. After removing the solvent under reduced pressure, the unreacted reactant was distilled under vacuum (5 × 10^{-2} mbar, 25°C). The remaining raw product was recrystallized in hexane. Yield: 20.31 g (76%) slightly yellow crystals.

^{1}H NMR (300.13 MHz, CDCl$_3$, δ): 8.72 (tr, J = 7.6 Hz, 2H), 8.38 (s, 1H), 8.30 (d, J = 8.1 Hz, 1H), 7.97 (d, J = 7.7 Hz, 1H), 7.72 (m, 3H), 7.63 (tr, J = 7.7 Hz, 2H), 7.53 (tr, J = 7.5 Hz, 1H), 7.40 (m, 3H), 3.71 (s, 6H); ^{13}C NMR (75.47 MHz, CDCl$_3$, δ): 139.09, 134.84, 134.76, 133.03, 131.81, 131.10, 130.52, 130.15, 129.50, 129.16, 128.94, 128.14, 127.95, 126.93, 126.76, 126.42, 123.08, 122.63, 51.15; ^{29}Si NMR (59.63 MHz, CDCl$_3$, δ): −27.69; Anal. calc. For C$_{22}$H$_{20}$O$_2$Si: C 76.73, H 5.90, N 0.00; found: C 76.71, H 5.85, N 0.00.

2.4 | General polymer synthesis

The synthetic procedures are based on reports of Mosley et al.[8] and Kim et al.[31,32]

To one equivalents of group A monomer, two equivalents of group B monomer and two equivalents of group C monomer, 13 equivalents of distilled water, eight equivalents of methanol are added. Depending on monomer A either concentrated hydrochloric acid (0.8 equivalents, for hydride containing polysiloxane) or tetra-*n*-butylammonium hydroxide (0.06 equivalents, for vinyl containing polysiloxane) are added (Figure 9). The flask was equipped with a distillation bridge to collect methanol and water. The suspension was stirred for 1 h at 85°C, for circa 1 h at 115°C. After no further solvent was distilled, the distillation equipment was removed, and the solution was stirred for an additional hour at 115°C. While the solution is cooling down, about 250 equivalents of toluene and 150 equivalents of water were added. After mixing the emulsion the water phase was removed. For the hydride containing polysiloxane the procedure was repeated with a concentrated solution of potassium bicarbonate and four times with water. For the vinyl containing solution the procedure was repeated two times with 2 M hydrochloric acid and three times with water. The organic phase was filtered with a 45 μm syringe filter and the solvent was removed under reduced pressure and then further removed under high vacuum for 4 h.

Group A: VP or HM.

Group B: 9-Phenanthrenylmethyldimethoxysilane (PHM) or 9-phenanthrenylphenyldimethoxysilane (PHP).

Group C: MM, methyldimethoxyphenylsilane (PM) or diphenylsiloxandiol (PP).

2.5 | Nomenclature

The synthesized polymers were named according to their consisting monomers (Figure 2). For the copolymer, the first letter is either "VP" or "HM" to indicate the type of the reactive side group. To show the condensation of the hydrosilylated solid polymer, it is named "CC" (instead of "VP" or "HM") to show the newly established —CH$_2$—CH$_2$— bridge. After the first letter, three letters
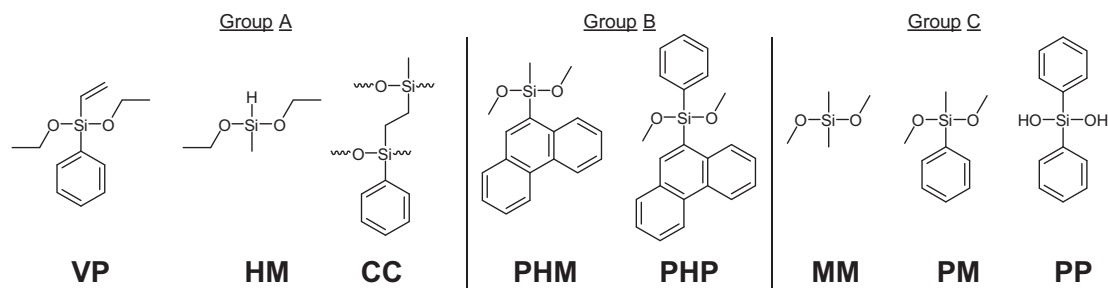

FIGURE 2 Overview of used monomers and their abbreviation. Group A shows the precursors for cross-linking and the cross-linked units; group B contains monomers that contain phenanthrenyl substituents; group C contains other monomers used to tailor the overall properties of the polysiloxanes

follow to indicate the highly aromatic side group at the silicon atom, "PH" (phenanthrenyl) with either a methyl (M) or phenyl (P) group attached. The two penultimate letters show the high-viscous monomer "MM" (dimethyl), "PM" (phenylmethyl) or "PP" (diphenyl). Additionally, after each monomer group, its percentage inside the polymer is also displayed.

2.6 | Curing of the polysiloxanes

The vinyl and corresponding hydride polysiloxane (each 330 mg) were mixed with Ossko platinum catalyst (6 ppm). To handle such low concentrations, the as received 2% Ossko catalyst in xylene was further diluted in xylene. The mixed copolymers were evacuated at 2 mbar for 1 h and doctor bladed with 120 µm onto a microscope slide. The slide was cleaned with isopropanol and acetone, and then plasma etched for 15 min. Finally, the films were cured at 100°C for 1 h and 150°C for 6 h to ensure complete cross-linking.

2.7 | General synthesis for end group capping

The polysiloxane (about 50 mg) was filled in a Schlenk flask, evacuated under high vacuum, and flooded with argon twice to create an inert atmosphere. Absolute THF (1.5 ml), *tert*-butyldimethylchlorosilane (40 mg, 0.26 mmol) and absolute triethylamine (100 µl) were added. After the solution was stirred for 18 h at 55°C the solvent was evaporated under high vacuum for 6 h.

3 | RESULTS AND DISCUSSION

3.1 | Monomers

Polysiloxane resins cured by Pt-catalyzed hydrosilylation are two-component systems consisting of a Si—vinyl and a Si—H containing copolymer. We prepared the polymers by polycondensation reactions of silicon alkoxide monomers. For the polymer preparation we used 1 equivalent of monomer of monomers containing cross-linking units (group A), 2 equivalents of monomers containing phenanthrenyl containing monomers (group B), and 2 equivalents of further monomers that influence the final properties of the polymer (group C, Figure 2). The monomer ratios were chosen because preliminary studies showed that 20% of the cross-linking monomer A is sufficient to obtain a solid material. Due to their low RI these monomers do not contribute to an overall increase of the RI and therefore only a minimal amount of should be used

if high-RI polysiloxanes are targeted. The amount of group B monomers should be as high as possible, but in some cases a value above 40% will lead to a fragile material. Monomers of group C complete to 100%, as they are relatively small and therefore mobile, which lowers the viscosity to obtain a processable material.

3.1.1 | Preparation and characterization of monomers

The dialkoxysilanes 9-phenanthrenylphenyl-dimethoxysilane and phenanthrenylmethyl-dimethoxysilane were synthesized in high yields applying a Grignard reaction between 9-bromophenanthrene and the appropriate alkoxysilanes[8,33,34] (Figure 3).

PHP formed a crystalline product immediately, while PHM was obtained as a colorless liquid, which crystallized after several months. The ^{1}H NMR spectra of both compounds showed the expected signals for the phenanthrenyl (9.0–7.5 ppm) and methoxy groups (4.0–3.5 ppm). 9-phenanthrenylphenyl-dimethoxysilane showed five additional protons in the aromatic region, while 9-phenanthrenyl-methyldimethoxysilane produces one signal in the methylsilane region (1.0 to −0.5 ppm). ^{13}C NMR revealed all theoretical signals in the expected region. ^{29}Si NMR was also used to determine if educts or side-products were present, which could be excluded due to the presence of only one signal (see spectroscopic data in the Supporting Information). The measured RI of phenanthrenylmethyldimethoxysilane was 1.6310.

We were able to obtain single crystal X-ray structures from the crystals obtained from PHM and 9-phenanthrenyldimethoxysilane (Figure 4, packaging
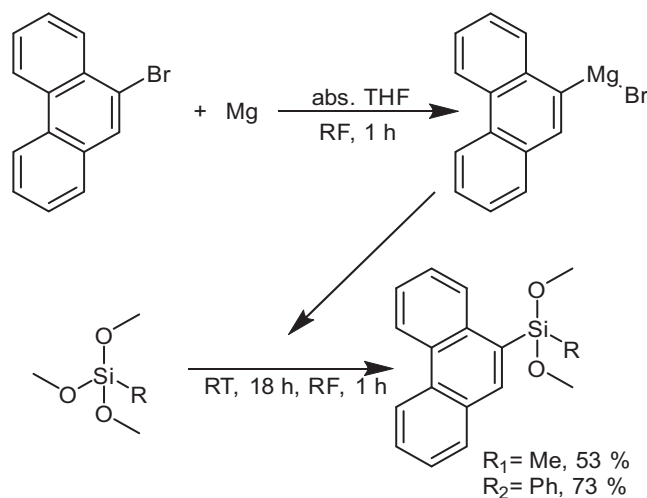

FIGURE 3 Grignard synthesis for dimethoxysilanes in THF. THF, tetrahydrofuran
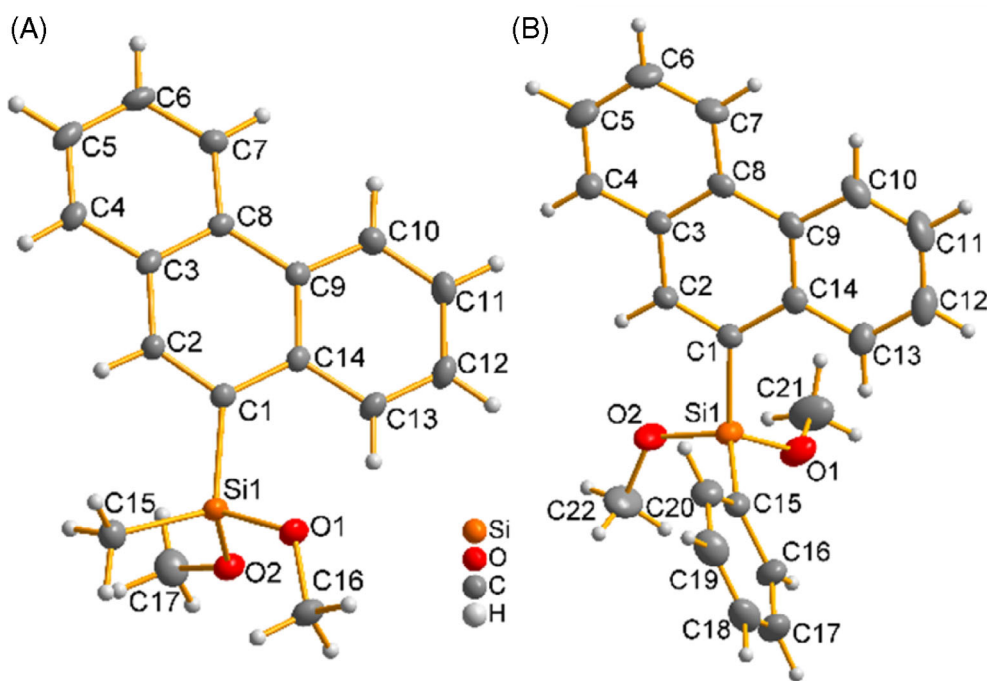
(A)

(B)

FIGURE 4 X-ray single crystal structure of (A) 9-phenanthrenylmethyldimethoxysilane and (B) 9-phenanthrenylphenyldimethoxysilane

	9-phenanthrenylmethyl-dimethoxysilane	9-phenanthrenylphenyl-dimethoxysilane
Si-C1(PH)	186.75(1) pm	186.52(11) pm
Si-C15(Me/Ph)	184.96(1) pm	185.57(12) pm
Si-O1	163.80(1) pm	162.81(10) pm
Si-O2	164.33(1) pm	163.11(10) pm
C1(PH)-Si-C15(Me/Ph)	111.705(2)°	113.37(5)°
C1(PH)-Si-O1	107.904(3)°	113.67(5)°
C1(PH)-Si-O2	109.330(3)°	102.72(5)°
C15(Me/Ph)-Si-O1	112.200(3)°	103.94(5)°
C15(Me/Ph)-Si-O2	109.676(3)°	112.49(5)°
O1-Si-O2	105.824(3)°	110.93(6)°
Torsion angle between planes: phenanthrenyl and Me/Ph	–	87.282(32)°

TABLE 1 Selected bond lengths and angles of (a) 9-phenanthrenylmethyl-dimethoxysilane and (b) 9-phenanthrenylphenyl-dimethoxysilane obtained by X-ray single crystal analysis

diagrams are reported in the Supporting information, supplementary crystallographic data can be obtained from Cambridge Crystallographic Data Centre as mentioned in the experimental part). The typical bond angles and distances of the crystal structures are reported in Table 1.

The bond length between the phenanthrenyl carbon atom (C1) and the silicon atom is marginally larger (186.8 pm for R = Me and 186.5 pm for R = Ph) than the usually observed Si—C bond (185 pm).[35] The bond length between the silicon atoms and each of the two oxygen atoms ranges from 162.8

to 164.3 pm, which is in the expected range of Si—O bond lengths.[36] The torsion angle between the two aromatic planes in 9-phenanthrenylphenyldimethoxy-silane of is 87.28°. The phenanthrenyl group shows an angle of 111.7° between the methyl and a higher angle of 113.4° between the sterically more demanding phenyl groups.

The metric of the crystalline structures is described in Table 2. While 9-phenanthrenyl-methyldimethoxysilane crystallizes in the monoclinic space group $P2_1/c$, 9-phenanthrenyl-phenyldimethoxysilane crystallizes in the orthorhombic space group $Pbca$.

TABLE 2 Crystal data of the synthesized monomers

Monomer	9-Phenanthrenyl-methyl-dimethoxy-silane	9-Phenanthrenyl-phenyl-dimethoxy-silane
Space group	$P2_1/c$ (14) monoclinic	$Pbca$ (61) orthorhombic
a (pm)	1013.11(3)	1029.28(8)
b (pm)	1531.34(5)	757.21(5)
c (pm)	2393.66(7)	1879.52(13)
β (°)	–	100.0991(36)
V (pm³)	1442.17(18)·10⁶	3713.56(20)·10⁶

TABLE 3 RIs of the used monomers measured in transmission mode at 20°C

Monomer	RI
Methyldiethoxysilane	1.3746
Vinylphenyldiethoxysilane	1.4795
Dimethyldimethoxysilane	1.3707
Methylphenyldimethoxysilane	1.4795
Diphenyldimethoxysilane (refers to used diphenylsilanediol [solid])	1.5440
9-Phenanthrenylmethyl-dimethoxysilane	1.6310
9-Phenanthrenylphenhyl-dimethoxysilane	n.a. (solid)

Abbreviation: RI, refractive index.

RIs of all monomers used in the polycondensation reaction were measured in transmission mode and are shown in Table 3.

The RIs of the group A monomers (Figure 2), HM and VP, are 1.3746 and 1.4795, respectively, which are relatively low compared to the synthesized new monomers. Group C monomers vary depending on the amount of methyl and phenyl groups, in the range of 1.3707–1.5440. Note that the polymerized diphenyl compound was diphenylsilanediol while for the RI comparison, diphenyldimethoxysilane was used because it is a liquid under ambient conditions. Substituting a methyl by a phenyl group increases the determined RI by 0.1088, while the second substitution only increases the value by 0.0645. The nonlinear increase results from the dimethoxy groups, which also have an impact and cannot be neglected. For the Group B monomers, only the RI of 9-phenanthrenyl-methyldimethoxysilane can be measured with a common Abbé refractometer as applied in our studies because 9-phenanthrenylphenyl-dimethoxysilane is a solid even at increased temperatures (∼80°C). The RI of 1.631 is superior to all other used monomers. It can be expected that the RI of the solid 9-phenanthrenylphenhyldimethoxysilane should even exceed this value.

3.2 | Polysiloxanes

The polysiloxanes were synthesized using a hydrolysis and condensation reaction of the alkoxide or diol monomers shown in Figure 2.[11,13,37–45] A typical synthetic strategy is shown in Figure 5.

From each group (A, B, and C, Figure 2) one type of monomer was selected in a specific amount and the monomers were mixed with 2.6 equiv. of water and 1.6 equiv. of methanol per silicon atom.[8] The type of catalyst was selected for the polymerization reactions depending on the composition of the monomers. For hydride containing group A monomers HCl was used, for vinyl group monomers tetra-n-butylammonium hydroxide was applied.[8] Hydride groups allow only an acid catalyzed polycondensation, because basic catalysis will lead to a loss of Si—H groups. Both acidic and basic catalysts can be used to polymerize the vinyl copolymer.[32,46–48]

### 3.2.1 | Characterization of linear copolymers

NMR measurements

All NMR measurements were carried out in chloroform-d, ¹H NMR spectra were referenced to the toluene CH₃ signal. The ¹H, ¹³C, and ²⁹Si NMR spectra are presented in the supporting information (Figures S3–S50). The ¹H NMR study reveals the signals of the methyl (1.0 to −0.5 ppm), hydride (5.3–4.5 ppm), and phenanthrenyl (8.8–7.0 ppm) groups. In ¹³C NMR both signal regions of methyl (2.0–1.0 ppm) and phenanthrenyl (138.0–122.5 ppm) are visible. In the ²⁹Si NMR there are four areas of D signals, the signals from −17.4 to −18.4 ppm can be assigned to methylsilane and the signals from −19.6 to −21.4 ppm are referring to dimethylsilane. From −31.3 to −33.2 ppm signals for phenanthrenylmethylsilane in the center of the polymer chain can be identified while the signals from −35.5 to −37.0 ppm refer to phenanthrenylmethylsilane close to the end of the polymer chain,[32] implying the slower reactivity of phenanthrenylmethylsilane in comparison to methylsilane or dimethylsilane. For the other copolymer, the ²⁹Si signals of the phenylmethyl groups are located at −33.0 ppm,[33] the vinylphenyl and diphenyl groups are present at −42 to −46 ppm.[33,34,49] The phenanthrenylphenyl signal is located at −45 to −50 ppm.

FTIR spectra

FTIR spectra were measured for all vinyl and hydride copolymers as well as the cured polysiloxanes. Here we display only the spectra for XX20_PHP40_MM40 (poly-, hydride-, and vinylphenanthrenylphenyldimethylsiloxane) (Figure 6). All other spectra can be found in the supporting information (Figures S51–S58). Characteristic IR signals of the
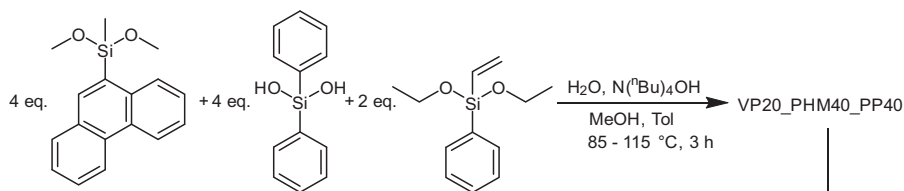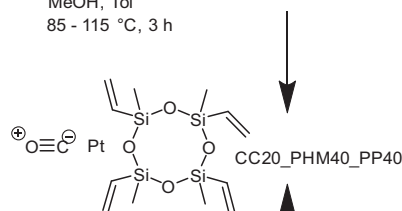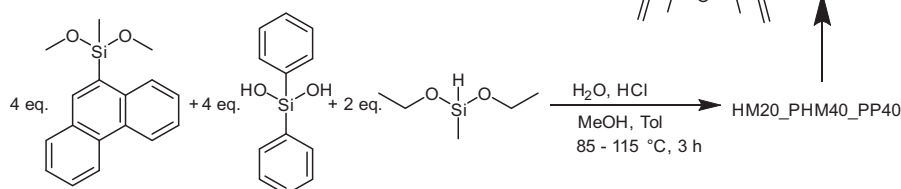
FIGURE 5 Exemplary synthesis of polyphenanthrenylmethyldiphenylsiloxane (CC20_PHM40_PP40) showing general polycondensation for hydride and vinyl copolymer and the hydrosilylation reaction using a platinum catalyst ("Ossko"). PHM, 9-Phenanthrenylmethyldimethoxysilane; PP, diphenylsiloxandiol
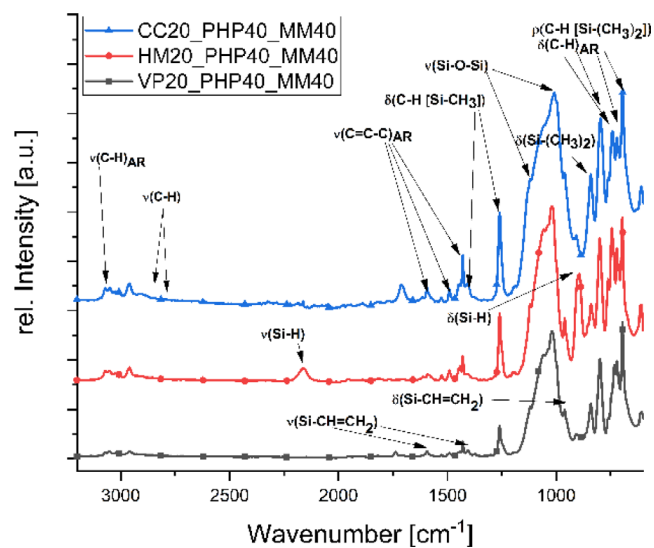

FIGURE 6 FTIR spectra of vinyl, hydride and hydrosilylated polyphenanthrenylphenyl-dimethylsiloxane (XX20_PHP40_MM40). FTIR, Fourier transform infrared; MM, dimethyldimethoxysilane; PHP, 9-phenanthrenylphenyldimethoxysilane

polysiloxane are 1120 and 1020 cm^{-1} for the Si—O backbone.[11,37–41,47,48] All other vibrations for the methyl, aryl and Si—H groups are in the expected regions.[11,37–41,47,48]

Molecular weight–SEC/NMR

The molecular weights of the linear vinyl and hydride copolymer were estimated applying ^{1}H NMR spectroscopy and SEC. For the ^{1}H NMR, the synthesized polysiloxanes were treated with *tert*-butyldimethylchlorosilane as an end-capping agent, which can easily be detected in the spectra (Figure 7). The chemical shift of the methyl groups in this end-capping substituents are in the region of 0.9–1.0 ppm. Therefore, they are not interfering with any other substituents in the polymer. Proton integration under assumption that the *tert*-butyl groups are only located at the end allows the determination of a rough estimation of the polymer mass. The thus calculated average molecular weights vary from 6 to 41 kDa (Table 4). The molecular weight of the vinyl copolymer is higher or similar to the mass of hydride copolymer and their SEC values range between 800 and 22.000 Da. Nearly all values are significantly lower than estimated by NMR spectroscopy. It has to be mentioned that the SEC method as a relative determination of molecular weight compared to a calibration standard has some limitations regarding molecular weight determination in case of the obtained polymers. Absolute molecular weight measurement was not possible with our instrumentation and the SEC instrument. The obtained SEC results are calibrated to a polystyrene standard. NMR as well as SEC measurements also have some challenges in the detection of cyclic derivatives, which are often formed during polycondensation of dialkoxysilanes. Therefore, the molecular weights given here must be handled with great caution.

The comparison of the SEC analysis of hydride and phenanthrenylmethyl containing polymer (HM20_PHM40_XX40) shows a rapid decrease of M_W and *PDI* with increasing the size of the group C monomer, which can result from increased activation energy due to steric hindrance. While the vinyl and phenanthrenyl-methyl containing polysiloxanes (VP20_PHM40_XX40) display a small M_W for the dimethyl
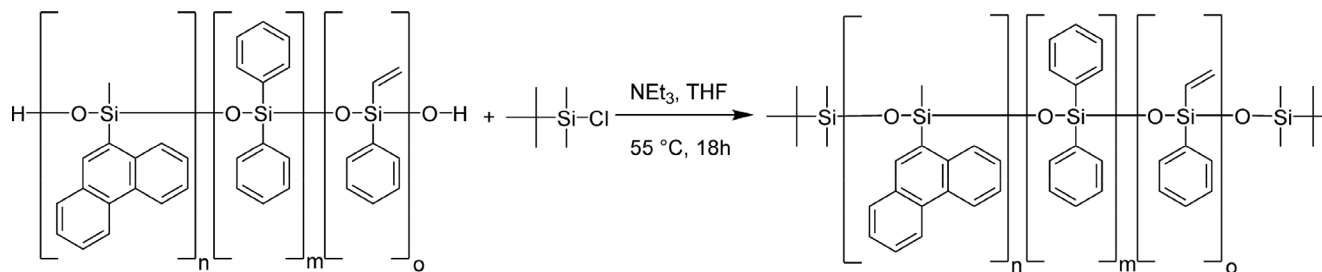
FIGURE 7 End group capping reaction of polyvinylphenylphenanthrenylmethyldiphenylsiloxane (VP20_PHM40_PP40) using *tert*-butyldimethylchlorosilane. PHM, 9-Phenanthrenylmethyldimethoxysilane; PP, diphenylsiloxandiol

TABLE 4 M_W and *PDI* of hydride and vinyl copolymer using ^{1}H NMR integration and SEC measurements

Hydride	M_W (g Mol^{-1}) NMR	M_W (g Mol^{-1}) SEC	*PDI* SEC	Vinyl	M_W (g Mol^{-1}) NMR	M_W (g Mol^{-1}) SEC	*PDI* SEC
HM20_PHM40_MM40	27,200	21,900	3.12	VP20_PHM40_MM40	2200	2500	1.24
HM20_PHM40_PM40	8300	6300	1.74	VP20_PHM40_PM40	35,200	8900	2.76
HM20_PHM40_PP40	15,200	1200	1.26	VP20_PHM40_PP40	18,800	8300	2.38
HM20_PHP40_MM40	6200	11,800	3.05	VP20_PHP40_MM40	27,100	12,100	2.68
HM20_PHP40_PM40	9100	3100	1.44	VP20_PHP40_PM40	8800	800	1.09
HM20_PHP40_PP40	10,100	11,900	3.67	VP20_PHP40_PP40	12,800	1100	1.20
HM40_PHM20_PP40	9500	3400	1.43	VP40_PHM20_PP40	13,900	2700	1.38
HM40_PHM40_PP20	40,700	4900	1.50	VP40_PHM40_PP20	27,300	3000	1.47

Abbreviations: HM, methyldiethoxysilane; MM, dimethyldimethoxysilane; PHM, 9-Phenanthrenylmethyldimethoxysilane; PHP, 9-phenanthrenylphenyldimethoxysilane; PP, diphenylsiloxandiol; RI, refractive index.

monomer, methylphenyl, and diphenyl monomers have very similar molecular weights. The comparison of HM20_PHP40_XX40 shows an increasing M_W in ^{1}H NMR studies from smaller to larger group C monomers, but in SEC measurements the dimethyl and diphenyl containing copolymers show the highest values. The M_W's and *PDI*'s of VP20_PHP40_XX40 decrease with increasing size of the group C monomer. The variation of the composition of HMxx_PHMxx_PPxx and VPxx_PHMxx_PPxx shows the smallest M_W and *PDI* for the 20% H containing sample, and the highest M_W and *PDI* for the 20% VP containing sample. For the vinyl and hydride polysiloxanes containing low amounts of phenanthrenylmethyl (PHM) or diphenyl (PP), M_W as well as *PDI* increase with PHM amount (40% PHM) and decrease with PP (40% PP) amount. Overall, the observed results are difficult to interpret because of the chemical different monomers and catalysts, as well as the variations in the detection of different species with the two methods.

Refractive indices

RIs of the polymers were determined in transmission mode and vary from 1.52 to 1.63 (Table 5). All values, despite for PHP with PM or PP, are higher for the hydride copolymer. The RI depends both on molar refraction and molar volume. Although the aromatic systems display a higher molar refraction smaller groups like hydride or methyl can sometimes lead to a denser packing of the chains, which is most likely the effect of the higher RI of the hydride and methyl substituted systems compared to the VP. Clearly the highest impact on the RI is observed by the phenanthrenyl groups.

Thermogravimetric analysis

TGA was carried out for each vinyl and hydride polysiloxane under oxygen and under nitrogen atmosphere up to 900 and 1000°C, respectively (all curves are displayed in supporting information). The two different conditions in the TGA analyses help to understand the difference between the depolymerization of the polysiloxanes (inert atmosphere) and the pyrolytic decomposition (oxidative atmosphere) of the organic groups. Up to 900°C the measurements were carried out under inert gas and at 900°C an oxygen atmosphere was applied to decompose pyrolytically formed graphite and oxidize all silicon moieties to SiO$_2$. The T_{95} value was used as starting point to compare all measurements, which is the temperature at 5% mass loss.[42–45] Values for the hydride and vinyl copolymer are

TABLE 5 RI's of hydride and vinyl copolymer measured in transmission mode at 20°C

Hydride	RI	Vinyl	RI
HM20_PHM40_MM40	1.593	VP20_PHM 40_MM40	1.521
HM20_PHM40_PM40	1.612	VP20_PHM 40_PM40	1.569
HM20_PHM40_PP40	1.627	VP20_PHM 40_PP40	1.578
HM20_PHP40_MM40	1.602	VP20_PHP 40_MM40	1.573
HM20_PHP40_PM40	1.618	VP20_PHP 40_PM40	1.633
HM20_PHP40_PP40	1.603	VP20_PHP 40_PP40	1.630
HM40_PHM20_PP40	1.599	VP40_PHM 20_PP40	1.596
HM40_PHM40_PP20	1.616	VP40_PHM 40_PP20	1.576

Abbreviations: HM, methyldiethoxysilane; MM, dimethyldimethoxysilane; PHM, 9-Phenanthrenylmethyldimethoxysilane; PHP, 9-phenanthrenylphenyldimethoxysilane; PP, diphenylsiloxandiol; RI, refractive index.

TABLE 6 Temperatures of the hydride and vinyl polysiloxanes at 95% residual mass under oxygen and under nitrogen atmosphere

Hydride copolymer	T_{95} O_2 (°C)	T_{95} N_2 (°C)	Vinyl copolymer	T_{95} O_2 (°C)	T_{95} N_2 (°C)
HM20_PHM40_MM40	234	248	VP20_PHM 40_MM40	190	193
HM20_PHM40_PM40	254	228	VP20_PHM 40_PM40	202	207
HM20_PHM40_PP40	246	247	VP20_PHM 40_PP40	198	191
HM20_PHP40_MM40	221	237	VP20_PHP 40_MM40	213	202
HM20_PHP40_PM40	210	211	VP20_PHP 40_PM40	254	244
HM20_PHP40_PP40	184	184	VP20_PHP 40_PP40	193	177
HM40_PHM20_PP40	269	282	VP40_PHM 20_PP40	218	220
HM40_PHM40_PP20	218	224	VP40_PHM 40_PP20	202	202

Abbreviations: HM, methyldiethoxysilane; MM, dimethyldimethoxysilane; PHM, 9-Phenanthrenylmethyldimethoxysilane; PHP, 9-phenanthrenylphenyldimethoxysilane; PP, diphenylsiloxandiol.

shown in Table 6. Figure 8 shows exemplary the TGA curves for HM40_PHM40_PP20 and VP40_PHM40_PP20 (polyvinylphenanthrenyl-methyldiphenylsiloxane respectively poly-vinylphenanthrenylmethyldiphenylsiloxane).

T_{95} temperatures of all polymers are in the range of 160–250°C. These low values can be explained by two decomposition mechanisms named "intramolecular back biting decomposition" (IBBD) and "preliminary hydrolysis" (PLH).[50–52] PLH occurs when the terminal OH group of a linear polysiloxane reacts with the silicon atom inside its own chain to form a cyclotrisiloxane or a cyclotetrasiloxane. IBBD is similar, but the ring formation takes place inside the chain without opening it. These mechanisms occur already at quite low temperatures because of their low activation energy (167 kJ). Hydride polysiloxanes show a higher decomposition temperature than their corresponding vinyl polymers. An explanation can be the higher molecular weights of the Si—H group containing systems which directly influences the numbers of end-groups. Because depolymerization mechanisms of polysiloxanes are often starting at the
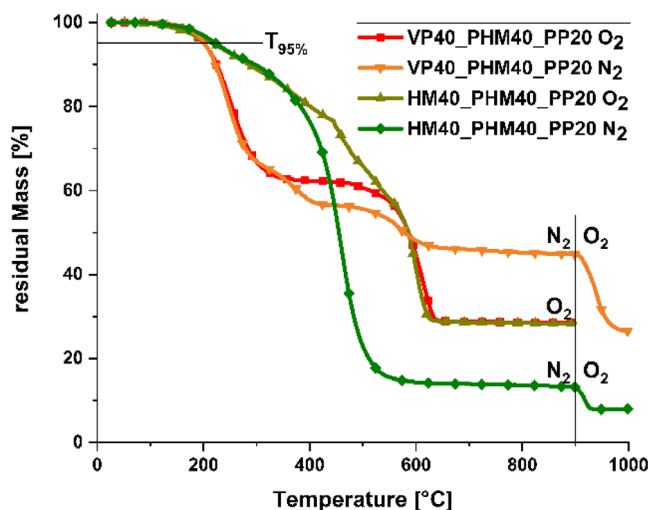

FIGURE 8 TGA measurements of VP40_PHM40_PP20 and HM40_PHM40_PP20 under nitrogen and oxygen atmosphere. HM, methyldiethoxysilane; MM, dimethyldimethoxysilane; PHM, 9-Phenanthrenylmethyldimethoxysilane; PP, diphenylsiloxandiol; TGA, thermogravimetric analyses
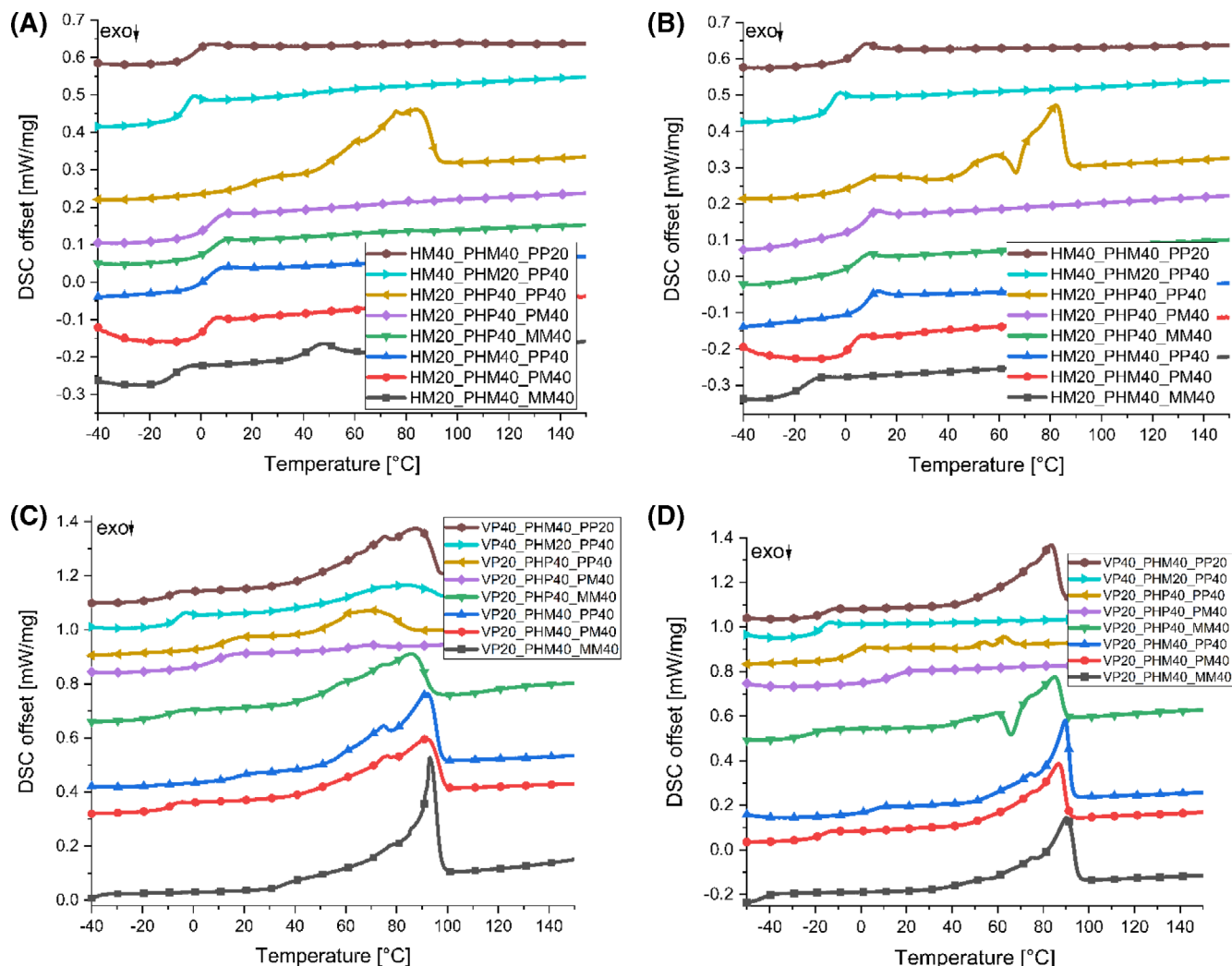
FIGURE 9 DSC curves of the first (A and C) and second (B and D) heating cycle of the hydride (A and B) and vinyl (C and D) copolymer. DSC, differential scanning calorimetry

chain ends a higher number can lead to accelerated decomposition. Under oxygen atmosphere the degradation of shorter or longer polymer chains shows no difference, under nitrogen atmosphere the smaller polymers show a higher onset temperature, because the unzipping mechanism is dominant (PLH, percentage more hydroxyl groups present). For longer polysiloxanes, the intramolecular backbiting (IBBD) is faster than the PLH and so determining.[53–56]

Differential scanning calorimetry

DSC measurements were carried out from −60 to 150°C in two cycles (Figure 9). The first heating cycle (Figure 9A,C) was used to determine melting temperature (T_m, Table 7) of crystalline areas inside the polysiloxanes. The second heating cycle (Figure 9B,D) was used to measure the glass transition temperature (T_g, Table 7) and additional melting temperatures which

could not be determined in the first heating cycle. Table 7 reports the T_m and T_g of hydride and vinyl copolymer as well as additional melting temperatures occurring in the second heating cycle (T_m 2 and T_m 3). T_m 3 is reported for completeness and, if observable, equals T_m 1 but with a much lower energy.

For VP20_PHP40_MM40, a second glass transition temperature was observed, indicating the existence of a kind of block-polymer structure[57–59] with a highly methyl side group containing region and a T_g of −22.3°C and a highly phenyl side group containing region with a T_g of 41.6°C. Overall, the glass transition temperature of the hydride compounds increases with increasing phenyl content from −17 to 7°C, while the T_g of vinyl copolymer ranges from −42 to 42°C. The only exception is VP20_PHP40_PP40 with a low T_g of −4.4°C. The vinyl polymers show a larger melting area compared to the hydride copolymer because the vinyl monomer consists of

TABLE 7 Melting and glass transition temperatures of hydride and vinyl copolymer

Homopolymere	Cycle 1		Cycle 2					
	$T_m 1$	Area (J g^{-1})	$T_g 1$	$T_g 2$	$T_m 2$	Area (J g^{-1})	$T_m 3$	Area (J g^{-1})
HM20_PHM40_MM40	47.07	3.30	17.19					
HM20_PHM40_PM40			2.10					
HM20_PHM40_PP40			6.98					
HM20_PHP40_MM40			3.31					
HM20_PHP40_PM40	81.39	0.04	6.75		12.54	0.39		
HM20_PHP40_PP40	83.68	24.49	4.24		58.80	3.71	82.21	12.89
HM40_PHM20_PP40			−6.55					
HM40_PHM40_PP20			3.50					
VP20_PHM 40_MM40	92.96	37.73	42.30		90.02	31.56		
VP20_PHM 40_PM40	91.46	30.32	18.35		86.65	26.04		
VP20_PHM 40_PP40	91.98	30.22	5.83		89.61	28.99		
VP20_PHP 40_MM40	85.89	27.52	22.30	41.57	59.84	1.31	84.71	14.92
VP20_PHP 40_PM40	67.98	0.82	14.14					
VP20_PHP 40_PP40	70.35	11.92	−4.39		54.07	0.40	62.88	1.04
VP40_PHM 20_PP40	83.38	7.51	18.23		−13.78	0.40		
VP40_PHM 40_PP20	87.29	31.33	17.21		83.35	27.72		

Abbreviations: HM, methyldiethoxysilane; MM, dimethyldimethoxysilane; PHM, 9-Phenanthrenylmethyldimethoxysilane; PHP, 9-phenanthrenylphenyldimethoxysilane; PP, diphenylsiloxandiol.

an additional phenyl group while the hydride monomer of an additional methyl group, which increases the T_g because of the lower degree of freedom of the sterically larger phenyl group. For the XXxx_PHMxx_PPxx copolymer with different composition, the highly aromatic ones (20% VP/HM) have the highest value, 7.0°C respectively 5.8°C, while the sterically least demanding (diphenyl compared to phenanthrenylmethyl) one (20% PHM) reveals the lowest values with −6.6 and −18.3°C, respectively.

3.2.2 | Characterization after curing

After purifying and drying the polysiloxane copolymer, the matched polymers (same monomers from group B and C in equal concentration) were cross-linked in a 1 H: 1 V mixture with Ossko platinum catalyst (Figure 9). Ossko catalyst was applied instead of the more commonly used Karstedt catalyst because a longer shelf life of the components can be expected due to higher activation energies for the curing. In addition, faster turnover number is obtained with Ossko catalyst at 150°C. The mixture will be evacuated at two mbar for 1 h and poured onto the desired substrate, for example a Teflon mold or a glass support. The polysiloxanes were cured at 100°C for 1 h and 150°C for 6 h.[8,11,32] Due to the small amount of platinum (6 ppm) longer curing times were necessary. The
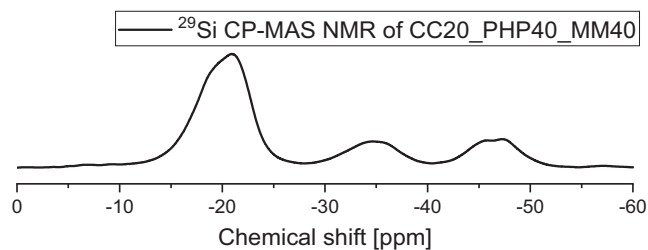

FIGURE 10 ^{29}Si CP-MAS NMR of CC20_PHP40_MM40. MM, dimethyldimethoxysilane; PHP, 9-phenanthrenylphenyldimethoxysilane

described procedure also decreases the formation of gas bubbles in the cured polymer. Figure 9 shows exemplarily the procedure for the production of CC20_PHM40_PP40 (polyphenanthrenylmethyldiphenylsiloxane). The received films are colorless and highly transparent (Figure 14). We systematically explored various compositions of monomers and different contents of A (HM or VP), B (PHM), and C (PP) in the production of the cross-linked polymers. For three batches, the amount of either A, B, or C was set to 20% while the remaining two were set at 40%, referring to the amount of silicon atoms.

Solid-state NMR
^{29}Si CP-MAS NMR was recorded for the cured sample CC20_PHP40_MM40 (Figure 10), the signal broadening

is related to the solid NMR measurement. The signal at −20 ppm can be referred to the dimethyl silicon atom[49,60–62] as well as the MeSi(OR)$_2$—CH$_2$—CH$_2$—X silicon atom[33,63] which was verified by ^{1}H ^{29}Si HMBC measurements of the HM20_PHP40_MM40 copolymer. The peak at −35 ppm is caused by the PhSi(OR)$_2$—CH$_2$—CH$_2$—X atom[33,34] which also was confirmed with ^{1}H ^{29}Si HMBC measurements of the VP20_PHP40_MM40 copolymer.

The signal at −47 ppm can be referred to the silicon atom of the self-synthesized phenanthrenyl-phenyl containing silicon atom.

FTIR spectra

FTIR spectra were measured from all cured polysiloxanes, only the spectra for XX20_PHP40_MM40 are displayed here (Figure 6), all other spectra can be found in the supporting information S51–S58. The characteristic IR signals of the cured polysiloxane are the same as the ones for the hydride and vinyl copolymer and were described earlier.[1] In the spectrum of the cured polysiloxane (PPHPMMS) signals at 2162 ν(Si—H) and 893 δ(Si—H) cm^{-1} as well as 1595, 1408 ν(Si—CH=CH$_2$) and 960 δ(Si—CH=CH$_2$) cm^{-1} can still be observed. Hence, no complete conversion was obtained during the hydrosilylation reactions. However, a rigid and non-sticky film was received. In accordance with other curing reactions of polysiloxanes, a full conversion cannot be achieved due to the increasing viscosity and reduced mobility during the hardening process.[8,46,64] Post-curing processes are possible with reactions of hydride groups in presence of platinum and oxygen or moisture.[65]

Thermogravimetric analysis

TGA measurements were carried out to analyze the thermal stability of the cured polysiloxanes (supporting information S59–S74). In Figure 11 a comparison of the onset temperatures at 95% residual mass of the different polymers is displayed. Overall, nearly all polysiloxanes reveal a higher decomposition temperature under nitrogen than the samples treated under oxygen.

The decomposition temperatures for the cured polysiloxanes under oxygen change from 300 to 370°C with increasing aromatic content. Under nitrogen the values vary from 300°C for the highly methyl containing polysiloxane to 420°C for the highly aromatic and phenanthrenyl-rich polysiloxane.[31,48,66] Besides the variation of monomers, different monomer contents for CCxx_PHMxx_PPxx (polyphenanthrenylmethyl-diphenylsiloxane) were also studied (Figure 11). The cured polysiloxanes show little difference in their decomposition behavior under oxygen atmosphere (336–350°C) and an increasing stability for the higher crosslinked polysiloxanes under nitrogen, while the increased phenanthrenyl-content excels the stability compared to a high-phenyl content. For lower aromatic content (<70% of

side-groups), the thermal stability is independent of the aromatic content (30–70%) with a T_{95} value of 300–350°C. With higher aromatic content, the thermal stability increases to 360–416°C.

Refractive index

RI of the cured polysiloxanes were measured in reflectance mode with a contact fluid (1-bromonaphthalene). The RI (Figure 12) varies from 1.57 to 1.63 for the cured
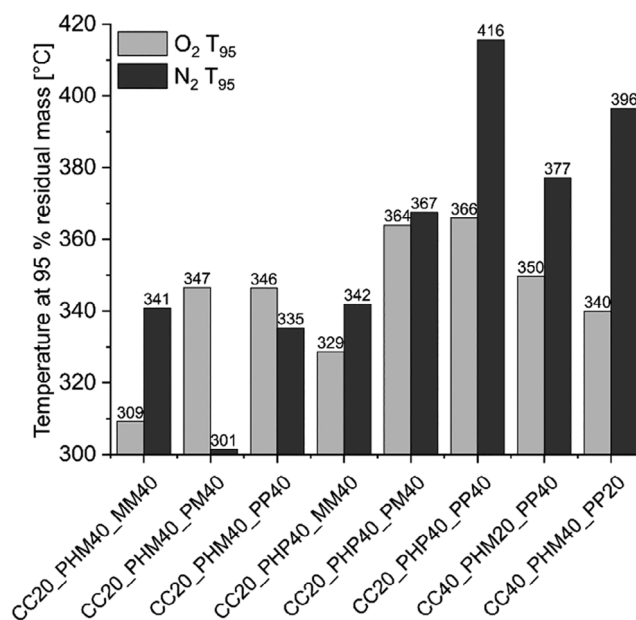

FIGURE 11 T_{95} values of the cured polysiloxanes under oxygen and nitrogen atmosphere
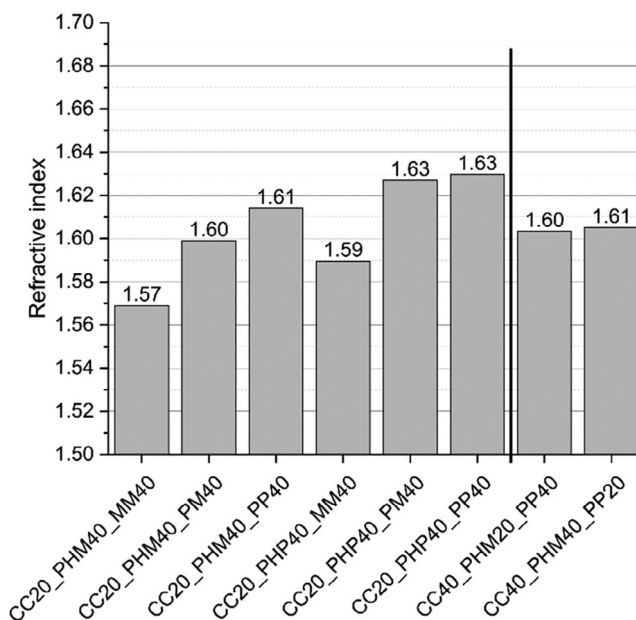

FIGURE 12 RI's of cured polysiloxanes measured in reflection mode at 20°C. RI's, refractive indices

polysiloxanes. With increasing phenyl content from CC20_PHM40_MM40 (0 Ph) < CC20_PHM40_ PM40 (1) = CC20_PHP40_MM40 (1) < CC20_ PHP40_PM40 (2) = CC20_PHM40_PP40 (2) < CC20_PHP40_PP40 (3), the RI increases from 1.57 to 1.63. Comparing the polysiloxanes with different monomer content, the one with the lowest number of cross-linkers (VP/HM) has the highest RI, while substituting PHM with PP shows little to no impact.

UV/Vis spectra–yellowness/whiteness index

The polysiloxanes were doctor bladed onto microscope slides (Figure 13) and analyzed with an integrating sphere in an UV/Vis spectrometer (Table 8). All polysiloxanes show a transmission from 96 up to 99%. Transmission decreases with increasing phenyl content and increasing RI.[3,67,68] The sample with only one aromatic group besides the phenyl one in the vinyl monomer (CC20_PHM40_MM40) reveals the highest value of
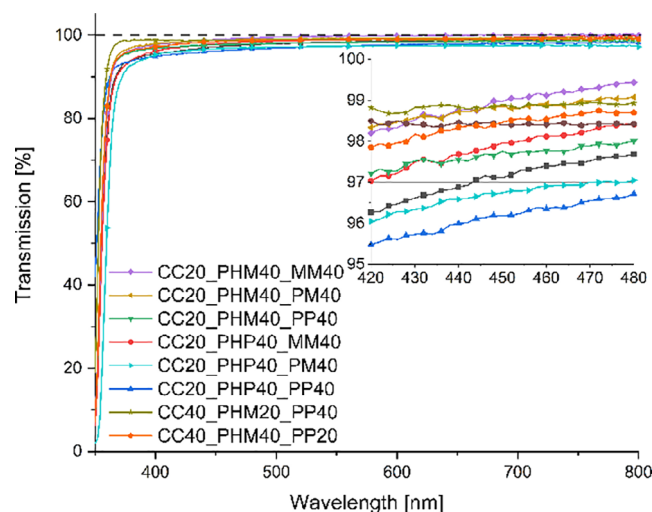

FIGURE 13 Transmission spectra of cured polysiloxanes

99.0%. Replacing one methyl group with a phenyl group (CC20_PHM40_PM40 & CC20_PHP40_MM40) reduces the transmission to 98.9% respectively 98.0%. By further increasing the aromatic content the transmission is reduced to 96.7% (CC20_PHP40_PM40) respectively 96.2% (CC20_PHP40_PP40). The same trend can also be observed when varying the composition of CC20_PHM40_PP40, the sample with the highest aromatic content shows the lowest transmission value (97.7% for 20% VH sample).

To evaluate the amount of light, which is diverted by passing through the samples, the haze value was calculated using Equation (3). In these calculations the transmission values were corrected by the glass slide.

$$Haze[\%] = \frac{diffusion\,[\%]}{corr.transmission\,[\%]} * 100. \qquad (3)$$

The haze value varies from 7.8 to 9.1% (at 450 nm) for the low phenyl containing polysiloxanes, while it increases up to 19% for the highly aromatic CC20_PHP40_PP40.

The whiteness and yellowness index (YI) were calculated using PerkinElmer UV Winlab software, the doctor bladed polysiloxane films are shown in Figure 14. Spectra were recorded from 380 to 780 nm using 5 nm step width. YI values larger than zero are implying yellowish probes, negative values bluish probes. A whiteness index (WI) value of 100 is achievable, higher values imply bluish and lower values yellowish samples. Measurements were carried out using international standards, ASTM D 1925–88 for YI and ASTM E 313–96 for WI.

YIs vary from −0.02 to 0.91 for nearly all synthesized samples, implying a slightly yellow color of the received films. However, these amounts are very small and can only barely be detected in thick films. Generally, the values are increasing with higher phenyl content.[69–73] Only two samples with the phenanthrenylphenyl containing monomer show higher values (1.14 for CC20_PHP40_MM40 and

TABLE 8 Transmission and haze values at 450 nm and yellowness and whiteness indexes of cured polysiloxanes

Polysiloxane	Transmission (%)	Haze (%)	Yellowness index	Whiteness index
CC20_PHM40_MM40	98.98	8.66	0.83	97.01
CC20_PHM40_PM40	98.86	7.79	0.60	97.51
CC20_PHM40_PP40	97.75	9.08	0.81	97.06
CC20_PHP40_MM40	97.96	7.96	1.14	97.01
CC20_PHP40_PM40	96.74	15.12	0.91	96.21
CC20_PHP40_PP40	96.18	18.77	1.67	93.58
CC40_PHM20_PP40	98.89	15.14	−0.02	98.74
CC40_PHM40_PP20	98.46	8.73	0.48	97.58

Abbreviations: MM, dimethyldimethoxysilane; PHM, 9-Phenanthrenylmethyldimethoxysilane; PHP, 9-phenanthrenylphenyldimethoxysilane; PP, diphenylsiloxandiol.
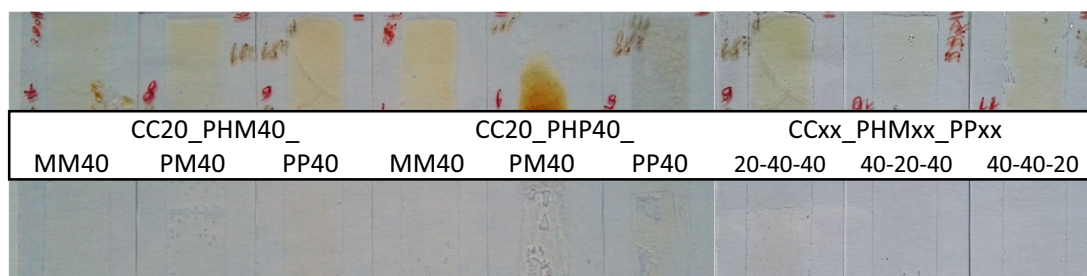
FIGURE 14 Transmission of polysiloxanes, bottom after synthesis, top after thermal treatment, from left to right: CC20_PHM40_MM40, CC20_PHM40_PM40, CC20_PHM40_PP40, CC20_PHP40_MM40, CC20_PHP40_PM40, CC20_PHP40_PP40, CC20_PHM40_PP40, CC40_PHM20_PP40, and CC40_PHM40_PP20. MM, dimethyldimethoxysilane; PHM, 9-Phenanthrenylmethyldimethoxysilane; PHP, 9-phenanthrenylphenyldimethoxysilane; PP, diphenylsiloxandiol
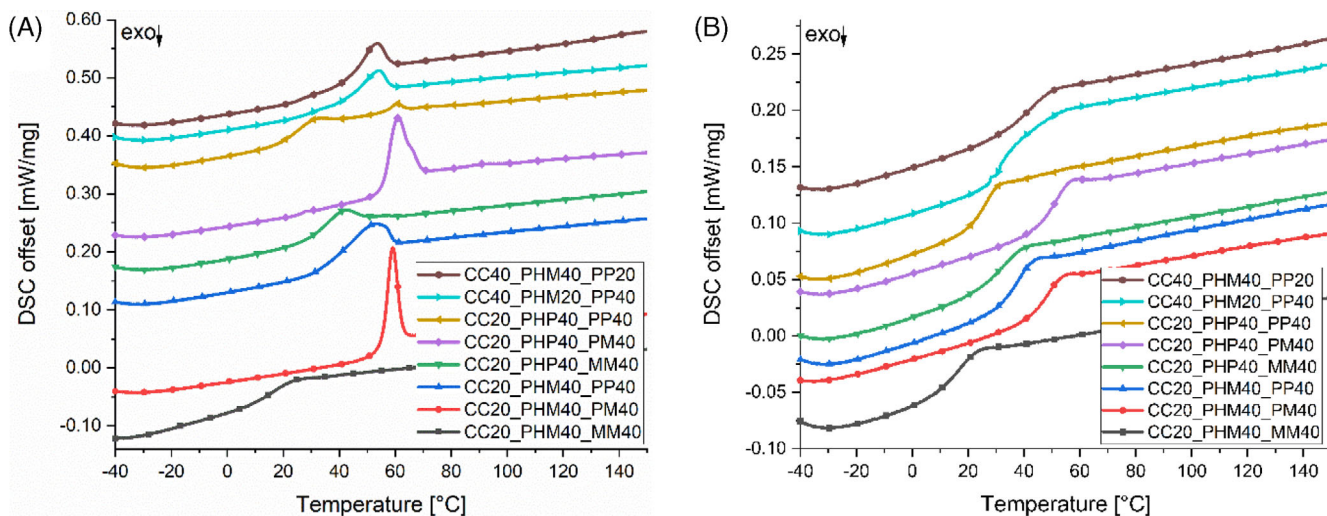

FIGURE 15 (A) First and (B) second heating cycle of DSC measurements of cured polysiloxanes. DSC, differential scanning calorimetry

TABLE 9 Differential scanning calorimetry of cured polysiloxanes

Cured polymer	T_m (°C)	T_m area (J g^{-1})	T_g (°C)
CC20_PHM40_MM40	–	–	17.01
CC20_PHM40_PM40	59.04	3.688	49.05
CC20_PHM40_PP40	52.54	2.597	39.25
CC20_PHP40_MM40	55.47	0.043	33.56
CC20_PHP40_PM40	61.31	3.956	51.33
CC20_PHP40_PP40	60.65	0.401	25.34
CC40_PHM20_PP40	53.59	2.014	34.68
CC40_PHM40_PP20	53.41	1.819	43.20

Abbreviations: MM, dimethyldimethoxysilane; PHM, 9-Phenanthrenylmethyldimethoxysilane; PHP, 9-phenanthrenylphenyldimethoxysilane; PP, diphenylsiloxandiol.

1.67 for CC20_PHP40_PP40). *WI* around 97 was observed for nearly all samples. The value can be increased using low amounts of phenyl and high amount of methyl groups in the polysiloxanes. Increasing the phenyl content lowers the *WI*, implying more yellowish films. The study using different amounts of monomers shows the best transmission and closest to 100 value for CC40_PHM20_PP40 with only 20% phenanthrenyl content. Clearly showing the direct correlation of delocalized electrons and the yellow color.
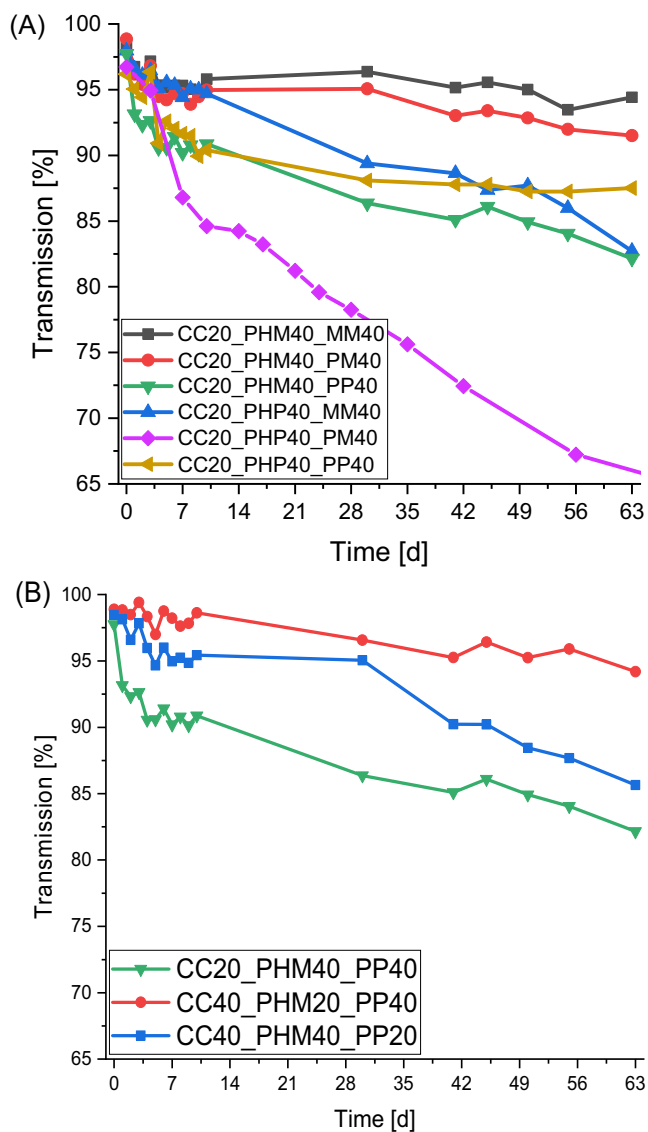
FIGURE 16 Transmission of synthesized polysiloxanes during thermal treatment at 180°C under air atmosphere

Differential scanning calorimetry

DSC measurements of the cured polysiloxanes were carried out from −60 to 150°C in two cycles analogously to the DSC measurements of the copolymer, the data for the first (a) and second (b) heating cycle are shown below (Figure 15). Curing generally increases the T_g.[74,75] The measurements of the cross-linked polymers were carried out although cross-linking decreases the ability of crystallization. Therefore, smaller or no signals are observed.[74–82] The method therefore can be used as an indirect measurement of cross-linking.[74,82] The integrated area decreases with increased cross-linking, also a shift of T_m to lower temperatures is visible.[78] The melting temperatures of the cured polysiloxanes (Figure 15, Table 9) are consequently lower than the ones of the vinyl copolymer with the same monomer composition,[78] this only

partially applies for the hydride copolymer. Some of the copolymer with higher amounts of methyl groups which contain PHM respectively MM monomers show a lower value. The T_m of all cured polysiloxanes varies between 9°C, a higher phenyl content leads by trend to higher values, whereas the polysiloxane with high concentrations of methyl groups (CC20_PHM40_MM40) shows no T_m. The T_g's of all cured polysiloxanes are significantly higher than their corresponding hydride and vinyl copolymer. T_g first ascends with increasing phenyl content from 17 to 51°C, except the polymer with the highest aromatic content which shows a value of 25°C. Varying the number of monomers shows no difference in T_m, while the T_g increases with increasing amount of sterically larger groups and lower amount of degrees of freedom: PP < VP/HM < PHM.

Aging test

To simulate the thermal aging inside the LED, the cured polysiloxanes were treated under operating temperatures of high-energy LEDs (150–200°C)[10] to test their thermal resistance. The thermal stability was verified by discoloration of the samples using UV/Vis measurements. The synthesized polysiloxanes, doctor-bladed onto a microscope slide, were thermally treated for 63 days at 180°C in air atmosphere (Figure 16). UV/Vis measurements were carried out regularly during this study (Figure 16). YI and WI were compared before and after the thermal treatment. The phenanthrenylmethyl containing samples show-decreasing transmission (Figure 16) after 63 days with increasing phenyl content (94.4% → 91.5% → 82.1%). The phenanthrenylphenyl containing polysiloxanes CC20_PHP40_MM40 and CC20_PHP40_PM40 lose transmission to 82.7 and 66.1%.

The varied composition of CC20_PHM40_PP40 shows decreasing transmission after 63 days with increasing phenyl content from 94.2% for 20% PHM over 85.7% for 20% PP down to 82.2% for 20% VH, which agrees with earlier results. The YI and WI implicate an intense yellowing of the polysiloxanes (Figure 17). With increasing phenyl content from CC20_PHM40_MM40 to CC20_PHM40_PP40 the yellowing increases linear, from 0.8 YI for the as synthesized polysiloxanes up to 18.7 YI and from 97 WI down to 42 WI.

The phenanthrenylphenyl samples CC20_PHP40_MM40 and CC20_PHP40_PM40 display high yellowing with increasing phenyl content, the YI increases from 1.1 (0.9) to 17 respectively 28 YI, the WI shows the same trend, it decreases form 97 (96) to 48 respectively 5.8 WI for CC20_PHP40_PM40. Interestingly, the sample with the highest phenyl content (CC20_PHP40 _PP40) shows little yellowing, comparable to the highly methyl containing sample CC20_PHM40_MM40. YI increases from 1.7 to 4.4, while WI decreases from 94 to 80. Varying the
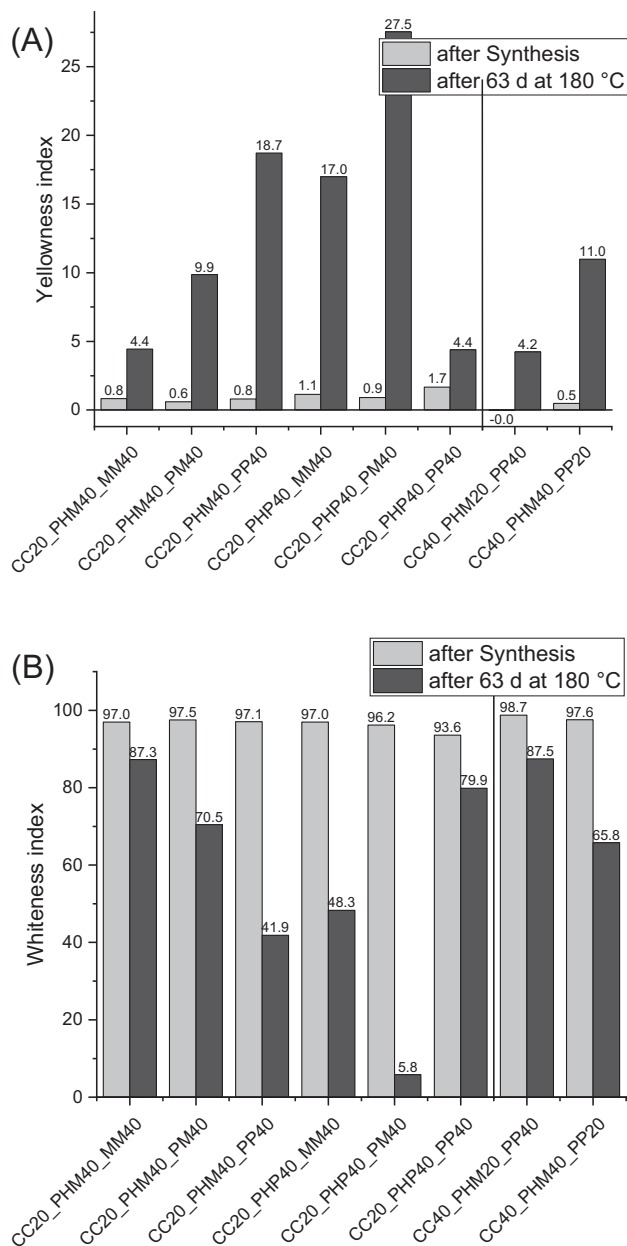
FIGURE 17 (A) Yellowness and (B) whiteness indices before and after thermal treatment at 180°C for 63 days under air atmosphere

composition of the monomers for CCxx_PHMxx_PPxx shows little to no difference (*YI* 0.0 to 0.8, *WI* 97.1 to 98.7) before the treatment. The yellowing also increases with increasing aromatic content from CCxx_PHMxx_PPxx with 20% PHM < 20% PP < 20% VH, indicating highly diphenyl < highly phenanthrenyl < highly diphenyl and phenanthrenyl content, from 4.2 over 11 to 19 *YI* and form 88 over 66 to 42 *WI*. The yellowing most likely occurs due to the formation of phenyl radicals, which are produced from cleaving from backbone chains.[7,69]

4 | CONCLUSIONS

Several novel high-RI polysiloxanes were fabricated using an acid respectively base catalyzed polycondensation approach to synthesize the linear hydride and vinyl copolymer out of newly synthesized arylic monomers. The resins show increasing RIs with increasing arylic content varying from 1.52 up to 1.63. These advanced copolymers were hydrosilylated using low amounts of platinum catalyst. The cured phenanthrenyl containing polysiloxanes show high-thermal stability under oxygen respectively inert atmosphere from 300 up to 420°C, which rises with increased arylic content and culminates in the CC20_PHP40_PP40 polymer. A tunable RI, which increases with rising aromatic content from 1.57 up to 1.63 can be fulfilled. A transmission over 96% could be achieved for all synthesized samples. It decreases from 99% for the highly methylic one to 96% for the highly arylic one. The glass transition temperatures can be tuned from 17 to 51°C with increasing the arylic and decreasing the methylic content. These outstanding properties are maintained for over 60 days under simulated LED operation temperatures at 180°C for all the polymers ranging from the high amounts of methyl containing ones (CC20_PHM40_MM40) to the high amounts of phenyl containing ones (CC20_PHP40_PP40). However, an increase of yellowing and whitening can be observed, which correlates with the number of aromatic groups in the polymers.

CONFLICT OF INTEREST
The authors declare no financial/commercial conflict of interest.

DATA AVAILABILITY STATEMENT
Additional data is available in the supporting information and upon request from the corresponding author.

ORCID
Volker Huch https://orcid.org/0000-0001-5337-5613
Guido Kickelbick https://orcid.org/0000-0001-6813-9269

REFERENCES

[1] Z. Ren, S. Yan, *Prog. Mater. Sci.* **2016**, *83*, 383.

[2] D. Sun, Z. Ren, M. R. Bryce, S. Yan, *J. Mater. Chem. C* **2015**, *3*, 9496.

[3] T. Higashihara, M. Ueda, *Macromolecules* **2015**, *48*, 1915.

[4] M. Ma, F. W. Mont, X. Yan, J. Cho, E. F. Schubert, G. B. Kim, C. Sone, *Opt. Express* **2011**, *19*, A1135.

[5] E. F. Schubert, *Light-Emitting Diodes*, Cambridge University Press, New York **2003**.

[6] D. W. Mosley, K. Auld, D. Conner, J. Gregory, X.-Q. Liu, A. Pedicini, D. Thorsen, M. Wills, G. Khanarian, E. S. Simon, *Proc. SPIE* **2008**, *6910*, 691017/691011.

[7] L.-B. Chang, K.-W. Pan, C.-Y. Yen, M.-J. Jeng, C.-T. Wu, S.-C. Hu, Y.-K. Kuo, *Thin Solid Films* **2014**, *570*, 496.

[8] D. W. Mosley, G. Khanarian, D. M. Conner, D. L. Thorsen, T. Zhang, M. Wills, *J. Appl. Polym. Sci.* **2014**, *131*, 39824.

[9] D. W. V. Krevelen, K. T. Nijenhuis, *Properties of Polymers: Their Correlation with Chemical Structure; their Numerical Estimation and Prediction from Additive Group Contributions*, Elsevier, New York **2009**.

[10] S. Watzke, P. Altieri-Weimar, *Microelectron. Reliab.* **2015**, *55*, 733.

[11] J.-S. Kim, S. C. Yang, S.-Y. Kwak, Y. Choi, K.-W. Paik, B.-S. Bae, *J. Mater. Chem.* **2012**, *22*, 7954.

[12] Y. Liu, X. Luan, X. Feng, X. Tan, Y. Han, X. Sun, *Polym. Adv. Technol.* **2017**, *28*, 1473.

[13] M. Zhao, Y. Feng, G. Li, Y. Li, Y. Wang, Y. Han, X. Sun, X. Tan, *Polym. Adv. Technol.* **2014**, *25*, 927.

[14] X. Yang, Q. Shao, L. Yang, X. Zhu, X. Hua, Q. Zheng, G. Song, G. Lai, *J. Appl. Polym. Sci.* **2013**, *127*, 1717.

[15] D. D. Li, S. Li, S. Zhang, X. W. Liu, C. P. Wong, *IEEE Trans. Compon., Packag., Manuf. Technol.* **2014**, *4*, 190.

[16] Y. Cheng, C. Lü, B. Yang, *Recent Patents Mater. Sci.* **2011**, *4*, 15.

[17] Y.-Y. Chang, B. Glorieux, C.-H. Hsu, C.-C. Sun, L.-Z. Yu, T.-H. Yang, T.-Y. Chung, *Opt. Mater.* **2016**, *55*, 55.

[18] P. T. Chung, S. H. Chiou, C. Y. Tseng, A. S. Chiang, *ACS Appl. Mater.* **2016**, *8*, 9986.

[19] Y. Lai, L. Jin, J. Hang, X. Sun, L. Shi, *J. Coat. Technol. Res.* **2015**, *12*, 1185.

[20] P.-C. Wang, C.-L. Lin, Y.-K. Su, P.-C. Chien, J.-H. Yeh, J.-K. Liou, C.-M. Wei, *Jpn. J. Appl. Phys* **2014**, *53*, 4.

[21] P.-C. Wang, Y.-K. Su, C.-L. Lin, G.-S. Huang, *IEEE Electron Device Lett.* **2014**, *35*, 657.

[22] J.-H. Huang, C.-P. Li, C.-W. Chang-Jian, K.-C. Lee, J.-H. Huang, *J. Taiwan Inst. Chem. Eng.* **2015**, *46*, 168.

[23] X. Hu, Z. Lin, Y. Zheng, Y. X. Asian, *J. Chem.* **2015**, *27*, 2905.

[24] Y. Sun, A. Gu, G. Liang, L. Yuan, *J. Appl. Polym. Sci.* **2011**, *121*, 2018.

[25] M. L. Lee, J. C. Kuei, N. W. Adams, B. J. Tarbet, M. Nishioka, B. A. Jones, J. S. Bradshaw, *J. Chromatogr.* **1984**, *302*, 303.

[26] W. B. Mefteh, H. Touzi, Y. Chevalier, H. B. Ouada, A. Othmane, R. Kalfat, N. Jaffrezic-Renault, *Sens. Actuator B Chem.* **2014**, *204*, 723.

[27] R. A. Domingues, I. V. r. P. Yoshida, T. D. Z. Atvars, *J. Polym. Sci. Pol. Phys.* **2010**, *48*, 74.

[28] Z. Lu, J. Ohshita, D. Tanaka, T. Mizumo, Y. Fujita, Y. Kunugi, *Compos. Interface* **2013**, *19*, 573.

[29] S.-I. Kondo, T. Harada, R. Tanaka, M. Unno, *Org. Lett.* **2006**, *8*, 4621.

[30] S.-i. Kondo, Y. Bie, M. Yamamura, *Org. Lett.* **2013**, *15*, 520.

[31] Y. H. Kim, Y.-W. Lim, D. Lee, Y. H. Kim, B.-S. Bae, *J. Mater. Chem. C* **2016**, *4*, 6.

[32] Y. H. Kim, J. Y. Bae, J. Jin, B. S. Bae, *ACS Appl. Mater.* **2014**, *6*, 3115.

[33] Q. Wu, M. Hetem, C. A. Cramers, J. A. Rijks, *J. High Resolut. Chromatogr.* **1990**, *13*, 811.

[34] G. Engelhardt, M. Mägi, E. Lippmaa, *J. Organomet. Chem.* **1973**, *54*, 115.

[35] D. R. Lide, *Tetrahedron* **1962**, *17*, 125.

[36] E. Prince, *International Tables for Crystallography*, Kluwer Academic Publishers, Dordrecht, Boston, London **2004**.

[37] P. J. Launer, B. Arkles, *Silicon Compounds: Silanes & Silicones*, Gelest, Inc, Morrisville, PA **2013**, p. 4.

[38] B. S. Furniss, A. J. Hannaford, P. W. G. Smith, A. R. Tatchell, *Vogel's - Textbook of Practical Organic Chemistry*, John Wiley & Sons, Inc, New York **1989**.

[39] A. L. Smith, *Spectrochim. Acta* **1960**, *16*, 87.

[40] A. Karlsson. Department of Polymer Technology, Royal Institute of Technology: Stockholm, **2003**, *107*.

[41] F. Delor-Jestin, N. S. Tomer, R. P. Singh, J. Lacoste, *e-Polymers* **2006**, *6*, 1.

[42] A. Kebritchi, M. Nekoomansh, F. Mohammadi, H. A. Khonakdar, *Polyolefins J.* **2014**, *1*, 117.

[43] D. E. Hegazy, *Arab J. Nucl. Sci. Appl.* **2014**, *47*, 112.

[44] R. Sahraeian, M. Esfandeh, S. A. Hashemi, *Polym. Polym. Compos.* **2013**, *21*, 243.

[45] H. Zhang, P. R. Westmoreland, R. J. Farris, E. B. Coughlin, A. Plichta, Z. K. Brzozowski, *Polymer* **2002**, *43*, 5463.

[46] J.-Y. Bae, Y.-H. Kim, H.-Y. Kim, Y.-B. Kim, J. Jin, B.-S. Bae, *ACS Appl. Mater.* **2015**, *7*, 1035.

[47] J.-S. Kim, S.-C. Yang, B.-S. Bae, *Chem. Mater.* **2010**, *22*, 3549.

[48] J.-Y. Bae, Y. Kim, H.-Y. Kim, Y.-W. Lim, B.-S. Bae, *RSC Adv.* **2013**, *3*, 8871.

[49] F. Uhlig, H. C. Marsmann, *Gelest Catalog.* **2008**, 208.

[50] P. R. Dvornic, R. G. Jones, W. Ando, *Silicon-Containing Polymers*, Dordrecht, Springer **2000**.

[51] I. Yilgor, E. Yilgor, *Polym. Bull.* **1998**, *40*, 525.

[52] M. A. Schiavon, S. U. A. Redondo, S. R. O. Pina, I. V. P. Yoshida, *J. Non-Cryst. Solids* **2002**, *304*, 92.

[53] A. Rucigaj, M. Krajnc, U. Sebenik, *Polym. Sci.* **2017**, *3*, 1.

[54] N. S. Tomer, F. Delor-Jestin, L. Frezet, J. Lacoste, *OJOPM* **2012**, *02*, 13.

[55] N. Grassie, S. R. Beattie, *Polym. Degrad. Stab.* **1983**, *9*, 23.

[56] S. R. Beattie, University of Glasgow, **1981**.

[57] M.-H. Yang, C. Chou, *J. Polym. Res.* **1994**, *1*, 305.

[58] M.-H. Yang, Y.-H. Hwang, J. C. Liu, C. Chou, *J. Chin. Chem. Soc.* **2001**, *48*, 1065.

[59] M.-H. Yang, W.-J. Huang, T.-C. Chien, C.-M. Chen, H.-Y. Chang, Y.-S. Chyan, C. Chou, *Polymer* **2001**, *42*, 8841.

[60] G. Engelhardt, H. Jancke, M. Mägi, T. Pehk, E. Lippmaa, *J. Organomet. Chem.* **1971**, *28*, 293.

[61] G. Engelhardt, H. Jancke, E. Lippmaa, A. Samoson, *J. Organomet. Chem.* **1981**, *210*, 295.

[62] G. W. Gray, W. D. Hawthorne, D. Lacey, M. S. White, J. A. Semlyen, *Liquid Crystals* **1989**, *6*, 503.

[63] I. R. Herbert, A. D. H. Clague, *Macromolecules* **1989**, *22*, 3267.

[64] T. C. Loh, C. M. Ng, R. N. Kumar, H. Ismail, Z. Ahmad, *J. Appl. Polym. Sci.* **2017**, *134*, 45285.

[65] X. Quan, *Polym. Eng. Sci.* **1989**, *29*, 1419.

[66] C. Chou, M.-H. Yang, *J. Therm. Anal. Calorim.* **1993**, *40*, 657.

[67] D.-H. Lee, S.-Y. Koo, H.-S. Lee, W. S. Kim, K. E. Min, L. S. Park, K. H. Seo, I. K. Kang, H.-J. Choi, *J. Appl. Polym. Sci.* **2002**, *85*, 38.

[68] R. Mercado, Y. Wang, T. Flaim, W. DiMenna, U. Senapati, *Proc. SPIE* **2004**, *5351*, 276.

[69] K.-H. Wu, K.-F. Cheng, C.-C. Yang, C.-P. Wang, C.-I. Liu, *Open J. Compos. Mater.* **2015**, *05*, 49.

[70] B. Riegler, R. Elgin, R. Thomaier, *Proc. SPIE* **2007**, 64780F.

[71] R. Elgin, B. Riegler, R. Thomaier, *Photonics Spectra* **2007**, *41*, 70.

[72] B. Riegler, R. Thomaier, S. Bruner, *Laser Focus World* **2006**, *42*, 115.

[73] B. Riegler, R. Thomaier. NuSil Lightspan Application Laboratory: IMAPS International Conference on Device Packaging, **2005**.

[74] W. J. Sichina, *Thermal Analysis*, PerkinElmer, Inc, Waltham, MA **2000**, p. 4.

[75] T. Dollase, H. W. Spiess, M. Gottlieb, R. Yerushalmi-Rozen, *Europhys. Lett.* **2002**, *60*, 390.

[76] J. A. Kerres, H. Strathmann, *J. Appl. Polym. Sci.* **1993**, *50*, 1405.

[77] A. Bac, D. Roizard, P. Lochon, J. Ghanbaja, *Macromol. Symp.* **1996**, *102*, 225.

[78] M. Baba, S. George, J. L. Gardette, J. Lacoste, *Polym. Int.* **2003**, *52*, 863.

[79] Z. Czech, K. Goracy, *Polimery-W.* **2005**, *50*, 762.

[80] Y. Karatas, N. Kaskhedikar, M. Burjanadze, H.-D. Wiemhöfer, *Macromol. Chem. Phys.* **2006**, *207*, 419.

[81] H. Li, J. Zhang, R. Xu, D. Yu, *J. Appl. Polym. Sci.* **2006**, *102*, 3848.

[82] F. Delor-Jestin, N. S. Tomer, R. Pal Singh, J. Lacoste, *Sci. Technol. Adv. Mater.* **2008**, *9*, 024406.

SUPPORTING INFORMATION

Additional supporting information may be found online in the Supporting Information section at the end of this article.

How to cite this article: D. Meier, V. Huch, G. Kickelbick, *J. Polym. Sci.* **2021**, *59*(20), 2265. https://doi.org/10.1002/pol.20210316